



Optimal enzyme allocation leads to the constrained enzyme hypothesis: The Soil Enzyme Steady Allocation Model (SESAM v3.1).

Thomas Wutzler¹, Christian Reimers¹, Bernhard Ahrens¹, and Marion Schrumpf¹

¹Max Planck Institute for Biogeochemistry, Hans-Knöll-Straße 10, 07745 Jena, Germany

Correspondence: Thomas Wutzler

(twutz@bgc-jena.mpg.de)

Abstract. Describing the coupling of nitrogen (N), phosphorus (P), and carbon (C) cycles of land ecosystems requires understanding microbial element use efficiencies of soil organic matter (SOM) decomposition. These efficiencies are studied by the soil enzyme steady allocation model (SESAM) at decadal scale. The model assumes that the soil microbial communities and their element use efficiencies develop towards an optimum where the growth of the entire community is maximized. Specifically, SESAM approximated this growth optimization by allocating resources to several SOM degrading enzymes proportional to the revenue of these enzymes, called the Relative approach. However, a rigorous mathematical treatment of this approximation has been lacking so far.

Therefore, in this study we derive explicit formulas of enzyme allocation that maximize total return from enzymatic processing, called the Optimal approach. Further, we derive another heuristic approach that prescribes the change of allocation without the need of deriving a formulation for the optimal allocation, called the Derivative approach. When comparing predictions across these approaches, we found that the Relative approach was a special case of the Optimal approach valid at sufficiently high microbial biomass. However, at low microbial biomass, it overestimated allocation to the enzymes having lower revenues compared to the Optimal approach. The Derivative-based allocation closely tracked the Optimal allocation.

The model finding that the Relative approach was a special case of the more rigorous Optimal approach together with observing the same patterns across optimization approaches increases our confidence into conclusions drawn from SESAM studies. Moreover, the new developments extend the range of conditions at which valid conclusions can be drawn. The new model finding that a smaller set of enzyme types was expressed at low microbial biomass led us to formulate the constrained enzyme hypothesis, which provides a complementary explanation why some substrates in soil are preserved over decades although often being decomposed within a few years in incubation experiments. This study shows how optimality considerations lead to simplified models, new insights and new hypotheses. It is another step in deriving a simple representation of an adaptive microbial community, which is required for coupled stoichiometric CNP dynamic models that are aimed to study decadal processes beyond ecosystem scale.



1 Introduction

The soil enzyme steady allocation model (SESAM) studies the effect of an adaptive soil microbial community on the coupling
25 of element cycles in aerated soils at decadal time scale. The coupling of the cycles of nitrogen (N), phosphorus (P), and carbon
(C) is especially strong in soils because the stoichiometric requirements of soil organic matter (SOM) decomposers is much less
flexible than the stoichiometric requirements of plants (Robert W. Sterner, 2002; Mooshammer et al., 2014b). Decomposer's
carbon use efficiency (CUE) are key to control how much of the litter input is stored in soil or respired again to the atmosphere
(Manzoni et al., 2017). Similarly, nitrogen use efficiency affects how much N in litter inputs is stored in organic matter or
30 mineralized and made available for plant nutrition (Mooshammer et al., 2014a). These element use efficiencies are affected by
stoichiometry of litter input and SOM, but also on properties of the microbial community. Furthermore, microbial community
is hypothesized to adapt to changing environment, such as increased litter inputs or litter stoichiometry or nitrogen deposition
(Manzoni, 2017; Manzoni et al., 2021).

However, there is a gap between knowledge of complex microbial ecology and community adaptations at the soil pore scale
35 and the purpose of dynamic SOM models to describe SOM changes at ecosystem to global scale and to integrate these SOM
models in Earth system models. We need to find ways to incorporate effects of soil microbial community adaptations on element
use efficiencies (Kaiser et al., 2014) without the need to model all the microbial populations and microbial details. The SESAM
model abstracts from microbial details by assuming that community composition develops towards maximizing growth of the
entire microbial community. The arguments why this optimality assumption is valid are rooted in systems ecology, which
40 focuses on the entire system rather than specific interactions. But this discussion goes beyond to scope of this manuscript and
here we assume that it is promising to explore the assumption that growth of the entire community is optimized.

One of the core ideas of SESAM is the optimization of community composition, in terms of enzyme allocation. SESAM
3.0, assumed the proportion of enzyme allocation into enzyme Z to be proportional to the revenue, i.e. return per investment,
of this given enzyme. But, the arguments why this approach is a heuristic for optimizing community growth given by Wutzler
45 et al. (2017, Appendix B) lack rigor. Therefore, a more rigorous mathematical treatment of these assumptions is required.

The developments of Wutzler et al. (2022), specifically the new formulation of decomposition based on quasi-steady state
of enzymes and the new formulation of revenue with limitation-weighted enzyme investments, make it possible to express the
revenue as a function of the enzyme allocation. This possibility allows us in this study to derive optimal community allocation
by maximizing the total return from enzymatic processing and to formulate two new optimality approaches.

50 The aim of this study is to present and compare the three approaches of computing enzyme allocation, i.e. Optimal, Relative,
and Derivative, at several scenarios of dynamic simulation and discuss the resulting insights and implications. One of those
insights derived in this study is the constrained enzyme hypothesis.



2 Methods

2.1 The SESAM model

55 SESAM is described in the previous paper of this incremental model description paper series (Wutzler et al., 2022). While the newly developed formulations of enzyme optimality are described in detail in the following sections, a short summary of the model is presented in this section.

Microbial biomass B produces enzymes that depolymerize substrate pools (labile L and residue R) that differ in their elemental ratios. Microbial community enzyme allocation α determines which part of the microbial community depolymerizes
60 L versus R by producing respective depolymerizing enzymes E_L , E_R , and biomineralizing enzyme E_P cleaving phosphate groups from the substrate. Microbes take up dissolved organic matter (DOM) and use it for synthesizing new biomass, new enzymes, or for catabolic respiration. A part of microbial turnover adds to the residue pool, another part is mineralized, and another part adds to DOM and is recycled into microbial biomass. Stoichiometric imbalance between DOM and B is resolved by mineralizing the excess element or immobilizing the required element (Φ_B) from inorganic pools (I). DOM and enzyme
65 pools are assumed to be in quasi-steady state at inter-annual simulation time scale.

2.2 Allocation optimization approaches

The optimum, to which microbial community in SESAM develops towards, is characterized by maximum growth of the entire microbial community, which in turn is achieved when the return from extracellular enzymatic processing is maximized. The return's currency is a weighted average of the returns of elements C, N, and P (Appendix C2). The weights in this average
70 correspond to the strength of the limitation of the growth of the microbial community by a respective element (Wutzler et al., 2022, eq. A15). The current limitation, in turn, is determined by the stoichiometry of different organic matter pools, the stoichiometric requirements of microbial growth, and depends on the enzyme allocation of the microbial community.

The derivative of the total return, u_T , with respect to each enzyme allocation share, α_Z , for short called 'the derivative' is the central quantity to inspect. The differences across those derivatives across enzymes determine the direction of changes
75 in enzyme allocation, i.e. changes in microbial community. Allocation is changed towards the enzyme Z with the highest derivative, i.e. highest increase in return per additional allocation, at the expense of decreasing allocation to enzymes lowest derivative. Hence, derivatives are equal at the optimum (Appendix C1). The derivatives decrease with increasing allocation because the return saturates at high enzyme levels. Therefore, it is often beneficial for the community to distribute investment into enzymes across different enzymes rather than investing solely into the enzyme with the highest potential return (Fig. 1).

80 The revenue of allocation to enzyme Z is another important quantity, because the product the revenue with allocation α_Z and total enzyme synthesis is equal to derivative of total return. The revenue is the return from enzymatic processing divided by the investment into enzyme production: $u_Z = \frac{d_{Z_w}(\alpha_Z)}{\alpha_Z \omega_{Enz} a_{EB}}$. The return, d_{Z_w} , is the elemental-limitation-weighted decomposition flux from the action of enzyme Z taken up by microbes (Appendix C2). The investment is the share, α_Z , invested into production of enzyme Z , multiplied by total elemental-limitation-weighted carbon flux allocated to enzyme production,
85 $\omega_{Enz} a_{EB}$.

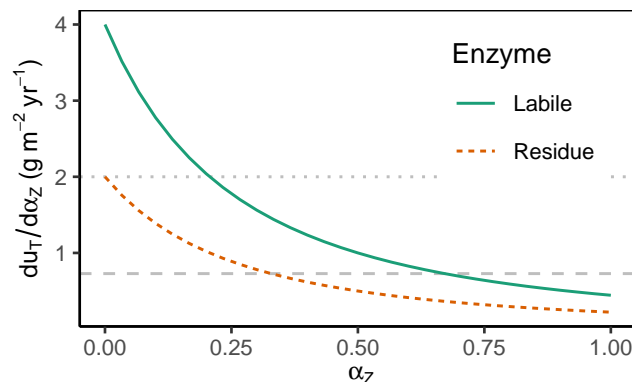


Figure 1. The derivative of total return with respect to enzyme allocation, $\frac{du_T}{d\alpha_Z}$, decreases with increasing share of allocation α_Z . Therefore, when increasing allocation proportions from zero until $\alpha_L + \alpha_R = 1$, in the shown example, microbes first increase allocation to labile enzymes, α_L , for which we here prescribed a higher potential return ($d_L = 2gm^{-2}yr^{-1}$, versus $d_R = 1gm^{-2}yr^{-1}$). Starting at levels $\alpha_L > 0.25$ (indicated by the dotted horizontal line crossing the labile derivative line), the increase in return with only increasing α_L is less or equal to the increase in return when also allocating something to residue degrading enzymes, $\alpha_R > 0$. Optimal allocation is attained when both derivatives are equal and allocation to both enzymes is increased until proportions add up to one (indicated by dashed horizontal line). This happens here at allocation about 1/3 to residue depolymerizing enzymes ($\alpha_R = 1/3$) and 2/3 to labile pool depolymerizing enzymes ($\alpha_L = 2/3$).

Hence total return and revenue depend on the potential decomposition flux, i.e. the amount and the decomposition rate of the substrate, as well as its stoichiometry via weighting by current elemental limitation of the microbes. In addition, they depend on enzyme levels, i.e. the size of the microbial biomass producing the enzymes, and on the current enzyme allocation, i.e. the shares of total enzyme production into the alternative enzymes. Potential return, d_Z , equals return unless excluding the factor that reduces return due to low enzyme levels, i.e. denotes the return potentially achieved at saturating enzymes.

Three approaches of estimating the time development enzyme allocation, α are presented in this study. The Optimal approach is the mathematically exact formulation of the hypothesis of maximum return of enzyme investment, but is only practical for simple cases. Therefore, two heuristic approximations are added. First, the Relative approach assumes that the optimal allocation can be estimated by setting the allocation proportional to the revenue. Second, the Derivative approach describes the direction of change in allocation without explicitly computing the optimal allocation.

2.2.1 Optimal approach

The Optimal approach computes the target allocation that maximizes total return by computing where the derivatives of total return across the set of allocated enzymes are equal (Appendix C1). Such a derivative of the return with respect to enzyme allocation α_Z is proportional to the derivative of the allocation times the revenue, $\frac{du_T}{d\alpha_Z} \propto \frac{d(\alpha_Z \text{ rev}_Z)}{d\alpha_Z}$. The revenue is an elemental-limitation-weighted return per enzyme investment, as explained in the previous section. While the maximum change of return



is realized at an arbitrarily small allocation $\rho_{Z_{max}} = \frac{d(\alpha_Z \text{rev}_Z)}{d\alpha_Z} \Big|_{\alpha_Z \rightarrow 0}$, the optimal allocation α^* often involves several enzymes (Fig. 1). However, if the maximum change of return for an enzyme Z_j is lower than the return of allocating only to other enzymes, the optimal allocation to this enzyme is zero, i.e. it is excluded from the set of allocated enzymes. The set of allocated enzymes, i.e. enzymes among which to distribute resources, can be found by the following algorithm.

105 1. Order the enzymes according to their maximum change in return, $\rho_{Z_{max}}$, index them by i , set $i = 1$ and start with a mix that includes only the most efficient enzyme $\{Z_1\}$.

2. Solve for the optimal allocation strategy α_i equalizing derivatives:

$$\frac{du_T}{d\alpha_Z} \propto \frac{d(\alpha_Z \text{rev}_Z)}{d\alpha_Z} = \rho_i \text{ for all } Z \in \{Z_1, \dots, Z_i\}$$

and allocate nothing to enzymes that are not part of the current mix.

3. If $\rho_i > \rho_{Z_{i+1max}}$ stop and report the found optimum $\alpha^* = \alpha_i$. Otherwise increase i , i.e. include enzyme Z_{i+1} in the mix and go to step 2.

110 Step 2 needs explicit solutions for different numbers and types of enzymes in the mix. Appendix C3 provides such explicit solutions for up to three enzymes across depolymerizing and biomineralizing enzymes.

2.2.2 Relative approach

The Relative approach, which was used up to SESAM version 3.0 (Wutzler et al., 2022), estimates optimal allocation to be proportional to revenue based on current allocation (1).

115
$$\alpha_{Z,Opt} = \frac{\text{rev}_Z}{\sum_i \text{rev}_i} \tag{1}$$

where rev_Z is the revenue for enzyme Z .

This study will show that it well approximates optimal allocation for the case of sufficiently high biomass levels (Appendix D).

2.2.3 Derivative approach

120 The Derivative approach computes the rate change of α_Z over time. It assumes that enzymes allocation changes faster, the larger the corresponding derivative is away from the average, i.e. the optimal state where all derivatives are equal. More precisely, it assumes the change rate to be proportional to $\frac{du_T}{d\alpha_Z} - \text{mean}_i \left(\frac{du_T}{d\alpha_i} \right)$ across the enzymes in the current mix (Appendix E). It does not rely on an optimal solution α^* . This is beneficial, because formulas in the Optimal approach for a higher number of enzymes or more types of enzymes quickly grow and involve higher-order polynomials of α_Z with multiple roots and
125 additional mathematically possible solutions outside the reasonable bound $\alpha_Z \in [0, 1]$.



The Derivative approach assumes that higher increase in total return lead to faster shifts of allocation towards this enzyme. It takes care, similar to the Optimal approach, to compute the average only across enzymes that are part of the current mix (Appendix E1).

2.3 Simulation experiments

130 In order to study the effects of using different allocation optimization approaches on model behavior, we set up different simulation experiments and compared differences in predictions among the approaches.

2.3.1 Prescribed potential returns

The Prescribed potential returns simulation experiment fixed the direct inputs to the function computing allocation changes. It neglected all other model feedback and focused and compared computation of optimum allocation for prescribed conditions.

135 Specifically, the experiment prescribed elemental-limitation-weighted potential return fluxes, d_Z (Appendix C2.1), which otherwise had been dynamically computed in the model from pools and parameters. It assigned values for enzymes decomposing residue litter and biomineralizing phosphorus of $d_R = 0.7$, $d_P = 0.5$, and varied the flux for enzymes decomposing labile substrates $d_L \in \{0 \dots 1\}$ in units $\text{g m}^{-2} \text{yr}^{-1}$. It simulated the allocation state until it converged to its estimated optimum for each d_L . For complete reference we list the other relevant parameters without further explanation
140 here: $a_E = 0.1$, $B = 1$, $e_P = 0$, $\tau = 365/30$, $k_{mN} = a_E B/2$, $\omega_{Enz} = 1$. The experiment included further runs with five-fold increased microbial biomass levels, B .

2.3.2 Decadal-term: FACE

The FACE simulation experiment simulated the decadal-term response of the system to increased labile carbon inputs. It started with model pools in steady-state with litter inputs. Next it prescribed a jump of labile carbon inputs by 20% simulated for 50
145 years and prescribed another jump of labile carbon inputs to initial values. It simulated N-limited conditions and excluded P-limitation by prescribing an arbitrary high value of potential P immobilization and very low P leaching (Table A2). The experiment included two more scenarios where parameters with the Relative approach had been adjusted to match the initial steady-state conditions of the Optimal approach. These scenarios allowed testing if the differences in predictions could be compensated by other model parameters.

150 2.3.3 Seasonal: Incubation

The Incubation simulation experiment amended a labile-depleted soil with a portion of labile litter and tracked the carbon use efficiency (CUE) of the microbial community over time and across different C:N ratios of the added labile organic matter. Specifically, it first simulated model pools in steady state with continuous annual inputs, then simulated no inputs for one year in order to deplete the labile pool, and next it simulated a step-increase of the labile C and N pools. In addition to the three

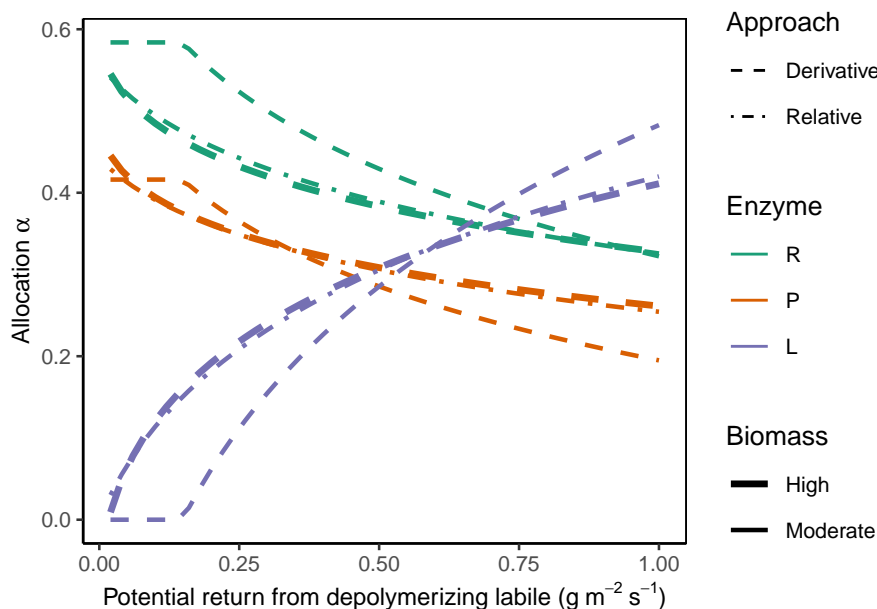


Figure 2. In the Prescribed potential returns simulation experiment, all allocation approaches predicted the same pattern of increasing allocation to enzyme, α_L with increasing potential return from depolymerizing labile OM and a corresponding decrease of allocation to the other enzymes, α_R and α_P respectively. The Derivative approach (dashed lines) and the Optimal approach (same predictions as Derivative, not shown) allocated nothing to the L depolymerizing enzyme at low potential returns at moderate microbial biomass levels. The Relative approach (dash-dotted lines) predicted very similar allocation as the Derivative approach at higher microbial biomass levels (indicated by overplotting of the thick lines), but overestimated allocation to enzymes of low revenue at moderate biomass levels (thin lines).

155 scenarios that differing by optimality approach, it simulated a scenario where microbial community allocation was fixed to $\alpha_R = 0.5$. This scenario allowed comparing results to a model where microbial community is not adaptive.

3 Results

3.1 Prescribed potential returns experiment

160 The Derivative approach yielded the same allocation as the Optimal approach with the Prescribed potential returns simulation experiment. The Relative approach yielded similar results as the Optimal approach for high microbial biomass levels, i.e. levels that resulted in an enzyme synthesis flux of 10 times the half-saturation constant of enzyme action k_{mN} . For moderate microbial biomass levels it overestimated allocation to the enzymes with low revenue (Fig. 2). With the Optimal and Derivate approaches there was no investment into enzymes with very low revenue at moderate biomass levels.

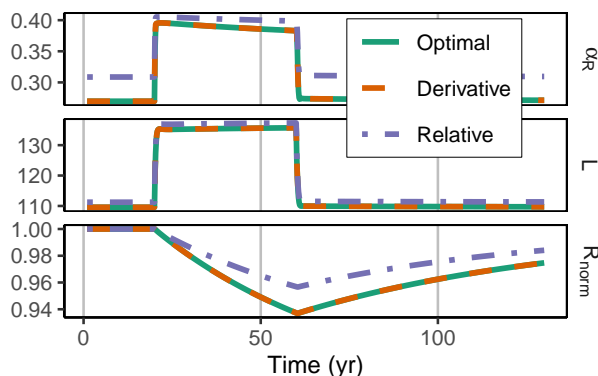


Figure 3. In the FACE simulation experiment all three allocation approaches predicted the same pattern of increased labile OM (L in $\text{gCm}^{-2}\text{yr}^{-1}$) and a shift towards mineralization of residue OM (R normalized by initial steady state values). The Derivative approach yielded the same predictions as the Optimal approach (indicated by dashed line overplotting the solid line). The Relative approach (dash-dotted line) slightly overestimated allocation to the residue degrading enzymes, α_R . This resulted in lower initial R stocks and a smaller decrease in the period of higher carbon inputs between year 10 and 60.

3.2 Decadal-term: FACE

165 The Derivative approach yielded the same allocation as the Optimal approach with the FACE simulation experiment. The Relative approach differed by overestimating the allocation to the enzyme with lowest revenue, α_R . Hence, it predicted smaller initial steady state stocks but also predicted relatively less mining of residue OM during period of increased carbon inputs (Fig. 3). With adjusting parameters related to organic matter decomposition in the simulation with the Relative approach, the same steady state stocks were simulated, but still the decrease of residue OM was smaller (Fig. B1).

170 3.3 Seasonal: Incubation

The difference between optimization approaches were small compared to the differences to the variant without adaptation (Fig. B2). All three optimization approaches showed decreased fluctuations of CUE, both in time, as well as across C:N ratios of added labile litter compared to a non-optimized fixed allocation. The Derivative approach's predictions matched the Optimal approach's predictions, while the Relative approach initially slightly underestimated allocation to the residue degrading enzyme (175 α_R) resulting in decreased biomass synthesis (Fig. 4).

The Relative approach's predictions differed from Optimal and Relative approach after one year of incubation when microbial biomass and enzyme levels declined (Fig. 5). It still allocated to the labile degrading enzymes ($\alpha_R < 1$), while with the Optimal approach, microbial community did not invest into degrading the small labile pool anymore. Hence, some of the labile pool was not decomposed, i.e. was apparently persistent with the Optimal approach.

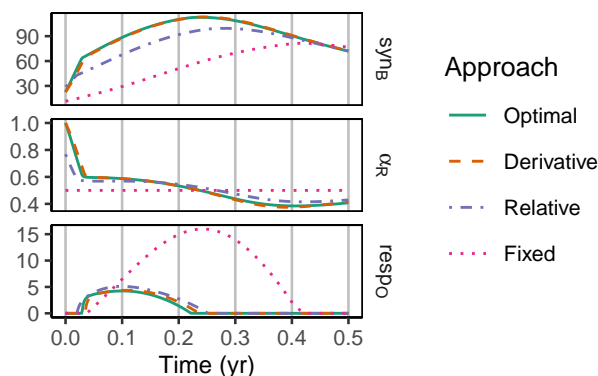


Figure 4. In the Incubation simulation experiment the three optimization approaches yielded a higher biomass synthesis, syn_B ($gCm^{-2}yr^{-1}$), than Fixed, i.e. not adapting allocation. They allocated relatively more resources to the residue degrading enzymes α_R during the initial N-limitation. This resulted in lower overflow respiration, $respo$ ($gCm^{-2}yr^{-1}$). The Relative approach initially underestimated α_R resulting in slightly lower biomass synthesis compared to the Optimal approach. Shown predictions correspond to an amendment with C:N ratio of 50 g/g.

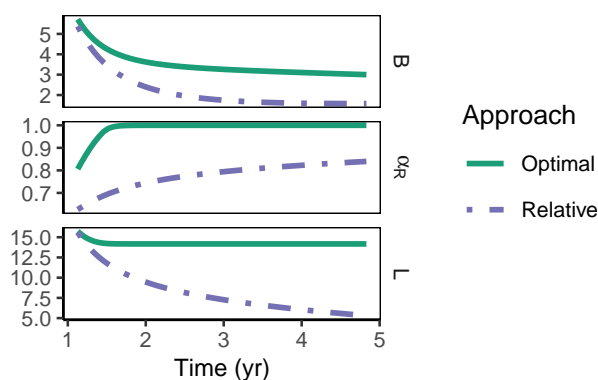


Figure 5. In the Incubation simulation experiment after some time microbial biomass, B (gCm^{-2}) decreased to low levels and allocation shifted towards Residue degrading enzymes only, $\alpha_R = 1$ with the Optimal approach (solid line). Hence, decomposition of a small remaining pool of labile organic matter, L (gCm^{-2}), stopped.

180 4 Discussion

The purpose of this work was to more rigorously define and implement the optimal growth hypothesis for SESAM and study the consequences of two simplifications. The finding that the previously used Revenue approach could be derived from the more rigorous Optimal approach for a set of conditions increases our confidence into conclusions drawn from SESAM studies.



The finding of no or only marginal differences between the Derivative and Optimal approaches encourages us to further develop
185 SESAM using the simpler Derivative approach.

4.1 Optimization approaches

The Optimal approach is the mathematical formalization of the hypothesis of community enzyme allocation optimizing mi-
crobial biomass growth for SESAM. The Relative approach, which has been used in previous SESAM versions, has been
shown in this study to be a special case of the mathematically formalized Optimal approach that is valid for enzyme allocation
190 fluxes larger than the half-saturation constant in the decomposition equation, which is usually valid at not too small microbial
biomass. The Derivative approach is another heuristic of optimal enzyme allocation that relies on derivatives of the enzyme
returns but does not require explicit formulas for the optimal allocation.

The three approaches predicted the same patterns in long-term as well as seasonal scale simulation experiments. Hence,
the conclusions drawn with SESAM so far were corroborated. Specifically, the following patterns emerge as a consequence
195 of microbial community adaptation of enzyme allocation: The priming effect (Kuzyakov et al., 2000) and the N banking
mechanism (Perveen et al., 2014), (Fig. 3), and the dampening of CUE fluctuations with an adaptive microbial biomass (Kaiser
et al., 2014) (Fig. B2).

While the Optimal approach is exact, it is tedious to implement and to update with further developments of SESAM. Explicit
formulas for the optimal allocation need to be derived for each combination of enzyme types in the mix of enzymes allocated
200 to. With including more enzymes or more types of enzymes, the formulas grow complex and an increasing number of potential
optima need to be checked and compared. Therefore, we also consider the simpler Relative and Derivative approaches and
discuss their effect on model predictions.

The Derivative approach yielded predictions that were so close to the predictions of the Optimal approach that they can
hardly be spotted in the plots (Figs. 3, 4). However, it works similar to gradient based numerical optimization schemes and
205 also shares its risks. First, it might result in limit cycles, where residue organic matter and microbial biomass oscillate instead
of converging to a stable optimal allocation. We argue that this actually may really happen in soil, although perturbations with
fluctuating litter input and decomposition fluxes changing with environmental conditions may quickly shift the decomposer
system into states away from the basin of such a limit cycle (Strogatz, 1994). If the Derivative approach yields predictions with
a decadal-scale limit cycle, perturbations of model drivers should help. Second, the Derivative approach might get stuck in local
210 optima and saddle points where the derivative of the return approaches zero. Gradient based optimization schemes implement
some notion of momentum to get past such points. There is also some momentum in the soil system, because enzyme levels
need some time to develop towards its quasi-steady state and microbes use storage compounds to support developments in
sub-seasonal periods where returns from enzymatic processing do not support further growth. Because SESAM explicitly tries
to abstract from such microbial details that are important for reacting on short-term fluctuations, the Derivative approach is
215 prone to this risk of getting stuck at saddle points. We did not encounter such conditions at our simulations yet. However, in
case such issues pose a problem, we need to think of ways how to implement simple notions of momentum in SESAM.

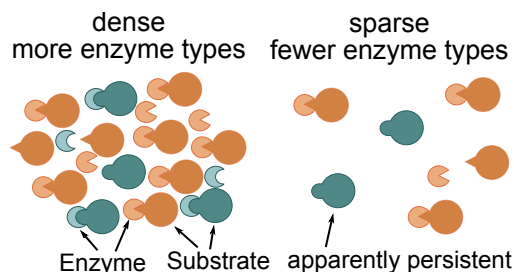


Figure 6. Constrained enzyme hypothesis: At low microbial concentrations, it is not beneficial for the microbial community to allocate to different enzymes types. Hence, some substrates, which may be quickly decomposed at higher microbial concentrations, become apparently persistent. This apparent persistence only indirectly depends on the properties and accessibility of the substrates and depends more on the relative availability of alternative substrates.

The Relative approach yielded predictions that differed from the predictions of the Optimal approach, specifically for low microbial biomass levels and for enzymes with low revenue. This was expected with the derivation of the conditions where the Relative approach is valid (Appendix D). Although small differences in enzyme allocation yield also only small differences in relative steady-state stocks, a small relative difference in the stock of the residue pool can result in considerable differences of total soil organic matter stocks. In the FACE simulation experiments (Fig. 3), the Relative approach predicted an initial share of enzyme allocation towards residue degrading enzymes of 30% compared to about 26% with the Optimal approach. This led to a decrease of residue steady state stocks from about 3600 to about 3400 gCm^{-2} (Fig. B1), which is an absolute difference that was larger than the entire labile pool. This in turn led to a predicted relative change of residue stocks with the FACE simulation experiment that significantly differed from the predictions with the Optimal approach (Fig. 3)

Based on these results, we will continue developing SESAM focusing on the Derivative approach.

4.2 The constrained enzyme hypothesis

The Optimal approach's predictions differed most from the previously used Relative approach's predictions at low microbial biomass levels. The Optimal approach excluded enzymes with low revenue from the set of enzymes to allocate to. For example, the allocation to the enzyme depolymerizing the labile pool was zero for a potential return of this enzyme below $0.2 \text{ g m}^{-2} \text{ yr}^{-1}$ in the Prescribed potential returns simulation (Fig. 2). The optimal enzyme allocation is determined primarily by availability of carbon and nutrients from organic and inorganic uptake. However, with the Optimal approach, the optimal enzyme allocation in addition depends on the size of the microbial biomass, because they control the relative size of the enzyme pools compared to saturating levels. The lower the microbial biomass, the farther away is enzyme production from levels where organic matter decomposition saturates. Hence at low microbial biomass it is not beneficial to distribute enzyme allocation across several enzymes including enzymes with low potential revenue. Similarly, the Optimal approach predicted in the Incubation simulation experiment that a small fraction of added organic matter, L is not decomposed (Fig. 5).



This insight into optimal allocation with SESAM generates an additional hypothesis why we observe high ages of some organic matter in soil and an additional insight into priming mechanisms (Fig. 6): Microbial community expresses a smaller set of enzyme types at low biomass levels. This non-investment into enzymes of relatively low revenue is a SOM preservation mechanism complementary to the existing hypotheses of chemical recalcitrance, physical protection by soil pores and by binding to minerals, and spatial separation of decomposers and substrate. It differs from the selective preservation hypothesis (Lehmann and Kleber, 2015) by making preservation dependent on the size or density of microbial biomass and by making preservation dependent on the availability of alternative substrates. When microbial biomass grows, e.g. by adding enough labile substrate, the focus on solely the enzymes with highest revenue is not beneficial any more and the optimal microbial community also invests into decomposition of the organic matter with lower revenue.

This hypothesis predicts that some organic matter is not decomposed in the presence of microbes that potentially can decompose it, if biomass levels are low and if there are alternative substrates decomposable with higher revenue. Further, the hypothesis predicts that also the old organic matter is decomposed at higher microbial biomass levels, e.g. at short-term substrate addition experiments or after disturbances when the microbial community can shortly grow on easily available substrates that are liberated with the disturbance.

4.3 Optimality assumptions

The conclusions of this paper depend on several assumptions. First, they depend on the formulation of depolymerization (Wutzler et al., 2022, eq. 2) (Appendix C2.1) and biomineralization (Appendix Fig C1). Specifically, they depend on the assumption that the decomposition fluxes saturate at high enzyme levels (Schimel and Weintraub, 2003; Tang and Riley, 2019). With alternative formulations (Wutzler and Reichstein, 2008) that assume a linear dependence of decomposition on enzyme levels (or alternatively microbial biomass) it would be optimal to allocate to the single enzyme that yields the highest decomposition flux of the currently limiting element.

Moreover, we assumed that the instantaneous growth rate of the microbial community is optimized. Alternatively, to instantaneous growth, the cumulative growth over a microbial characteristic time-span could be optimized, e.g. the time for decomposing a single portion of carbon (Manzoni et al., 2023). The instantaneous strategy is sub-optimal to dynamical strategies if legacy effects are present that are internal to the optimized system. At the same time the two strategies yield similar performance when legacy effects are external to the optimized system (Feng et al., 2022), because competition alters the trade-off between current and future gains. Hence, optimizing at a different system boundary, which is usually associated with a different time scale, results in different optimal strategies (Dewar, 2010). The focus of SESAM on the entire microbial community calls for a dynamic strategy because it renders many factors internal, compared to a focus on competing microbial populations that renders soil organic matter an external factor. However, SESAM is intended to model decadal-term changes and to be driven with annually averaged drivers. The two strategies will presumably converge at these conditions where enzyme pools and decomposition develop towards a quasi-steady state because current and future gains are similar within a seasonal timescale of microbial growth.



SESAM focused on the partitioning of allocation of the total enzyme investment towards different enzymes. In addition, the total allocation into enzyme production can be a trait that adapts to optimize microbial growth (Calabrese et al., 2022). Future SESAM developments will explore if a joint optimization of total allocation and allocation partitioning can be derived and whether such a joint optimization alters the consequences for the long-term dynamics of SOM stocks.

275 4.4 Observational evidendence

The constrained enzyme hypothesis is a consequence of several model assumptions. It was derived without reference to observed patterns. However, there is already some observational evidence supporting the hypothesis of lower diversity of expressed enzymes at low microbial activity.

Metatranscriptomics (Carvalhais et al., 2012) directly studies functional diversity of expressed enzymes in soils. Evidence
280 for the constrained enzyme hypothesis resulting from such studies are mixed. Straw amendmends increased microbial activity of an agricultural soil and upregulated several enzyme families and resulted in higher microbial diversity (Kozjek et al., 2023), supporting the constrained enzyme hypothesis. Contrary, straw amendmend resulted in a downregulation of enzyme families in an already diverse grassland soil in the same study.

A novel approach of combining isotopically labeled measurements of microbial growth with quantitative stable isotope
285 probing (Hungate et al., 2015) can assess microbial diversity of the active part of the microbial community. It revealed a reduction of diversity of actively growing microorganisms with lower microbial activity under drought (Richter, 2023), which is in line with expected reduction in diversity of expressed enzymes with lower microbial biomass as predicted with the constrained enzyme hypothesis.

Analysis of potential activities of specific enzymes (Marx et al., 2001) and its spatially resolved zymography version (Spohn
290 et al., 2013) do not directly tell about the diversity of enzyme expression, because only specific enzymes are analyzed. However, in line with the constrained hypothesis zymography of a temperate forest soil revealed that common enzymes are hardly expressed outside hotspots and before fostering microbial growth by amendmends (Heitkötter and Marschner, 2018).

In summary, studies that specifically look at enzyme diversity in relation to microbial biomass levels are still lacking. However, we can find observations from other studies that are in line with the constrained enzyme hypothesis.

295 5 Conclusions

The Optimal approach is the mathematical formulation of the hypothesis that microbial community enzyme allocation develops in a way that optimizes growth. The finding of similar predictions by the heuristic approaches compared to the Optimal approach increases our confidence into conclusions drawn with SESAM. The heuristic Relative approach is shown to be a special case of the Optimal approach valid at sufficiently high microbial biomass levels. The Derivative approach, another
300 heuristic of the Optimal approach, is valid also for low microbial biomass levels. Given that the Derivative approach is a good heuristic of the Optimal approach that is better scalable to more enzyme types than the Optimal approach, we will continue the SESAM developments with the Derivative approach.



The Optimal and Derivative approaches yield predictions at low microbial biomass that differ from the predictions of the Relative approach. Specifically, they predict that enzymes with low revenue are not expressed at low microbial biomass. This finding generated the constrained enzyme hypothesis for the preservation of organic matter in soils.

Code availability. SESAM (v3.1) is available coded in R at <https://github.com/bgctw/sesam> (last access: June 12th 2023) (doi: 10.5281/zenodo.8026318) and coded in Julia at <https://github.com/bgctw/Sesam.jl> (last access: June 12th 2023) (doi:10.5281/zenodo.8026366). R source code is released using the GPL-2 licence, because it uses other GPL libraries. Julia code is released using the more permissive MIT License.

The simulation experiments are part of the R repository. They use the derivSesam3P model variant. The Prescribed potential returns code is provided in "Allocation" section of file develop/23_optimAlloc/sesamess/sesam_LRP_deriv.Rmd. The Decadal-term FACE code is provided with file develop/23_optimAlloc/Face1_3P.Rmd. The Seasonal Incubation code is provided with file SimBareSoilPulse_opt.Rmd.

Appendix A: Symbols used

Tables A1, A2 and A3 list state variables, model drivers, model parameters and other symbols used in SESAM.

Symbol d with a subscript denotes a form of decomposition or return flux, while the symbol d without subscripts denotes the derivative operator.

Appendix B: Additional figures

This section provides figures that detail some of the results. First, predictions of the FACE simulations experiment for non-normalized residue pool, R , and for additional scenarios with adjusted decomposition parameters are shown in Fig. B1. Next, emergent carbon use efficiency (CUE) predicted by different approaches with the Incubation experiment are shown in Fig. B2.

Appendix C: Optimal enzyme allocation

This section derives explicit formulas of optimal enzyme allocation by finding the allocation that maximizes total return. It starts with a lemma that states conditions for which the optimum is attained when derivatives are equal. The lemma is then used in subsequent derivations of optimal allocation.

C1 Optima at equality of derivatives

Let $u_T(\alpha) = C_2 \sum_Z \alpha_Z \text{rev}_Z$ be a function that is a weighted sum of components rev_Z up to some constant $C_2 \neq 0$, where weights $\alpha_Z \in (0, 1)$ add up to one: $\sum_Z \alpha_Z = 1$ and component rev_Z may depend on weight α_Z but not on the other weights. Further, let rev_Z be differentiable to α_Z and let potential optima $\in (0, 1)$. Then at the optima of $u_T(\alpha)$ all derivatives $\frac{d(\alpha_Z \text{rev}_Z)}{d\alpha_Z}$ are equal.



Table A1. State variables and model drivers. Values correspond to FACE simulation experiment initial steady state for Optimal approach.

Symbol	Definition	Value	Unit
L, L_N, L_P	C, N, and P in labile substrate	$109 \cdot \beta_{E_{i_L}}(0)$	g m^{-2}
R, R_N, R_P	C, N, and P in residue substrate	$3687 \cdot \beta_{E_{i_R}}(0)$	g m^{-2}
B	Microbial biomass C	30.46	g m^{-2}
I_N	Inorganic N	0.194	g m^{-2}
I_P	Inorganic P	2157**	g m^{-2}
$\alpha_L, \alpha_C, \alpha_P$	Allocation to enzyme $Z \in \{L, R, P\}$	0.74, 0.26, 0.0	(-)
$i_L(t)$	labile C input	400.0	$\text{g m}^{-2}\text{yr}^{-1}$
$\beta_{N_{i_L}}(t)$	C/N ratio of labile inputs	28	g g^{-1}
$\beta_{N_{i_R}}(t)$	C/N ratio of residue inputs	10	g g^{-1}
$\beta_{P_{i_L}}(t)$	C/P ratio of labile inputs	120	g g^{-1}
$\beta_{P_{i_R}}(t)$	C/P ratio of residue inputs	40.3	g g^{-1}
$i_{I_N}(t)$	inorganic N input	0.0714	$\text{g m}^{-2}\text{yr}^{-1}$
$i_{I_P}(t)$	inorganic P input	0	$\text{g m}^{-2}\text{yr}^{-1}$
$k_{I_{EP}}(t)$	plant uptake of inorganic E per I_E	100*	yr^{-1}
$u_{I_E, \max}(t)$	max plant uptake of E	$= i_L / \beta_{E_{i_L}} + i_{I_E}^{**}$	$\text{g m}^{-2}\text{yr}^{-1}$

* arbitrary high value so that plant uptake is constraint by $u_{I_E, \max}(t)$

** balancing nutrient input to the system

Proof: Because of the sum-to-one constraint, we express one of the weights as a function of the other weights and have only $n - 1$ free weights.

$$\alpha_n = 1 - \sum_{Z=1}^{n-1} \alpha_Z$$

$$\frac{d\alpha_n}{d\alpha_Z} = -1$$

We are interested in the optima of u_T away from the borders, i.e. $\alpha_{\text{Opt}} \in (0, 1)$. In the derivative to α_Z all terms vanish except the term involving rev_Z and the term involving rev_n , because there α_n is a function of α_Z . By the chain rule we have:

$$\begin{aligned} \frac{du_T}{d\alpha_Z} = 0 &= C_2 \left(\frac{d(\alpha_Z \text{rev}_Z)}{d\alpha_Z} + \frac{d(\alpha_n \text{rev}_n)}{d\alpha_n} \frac{d\alpha_n}{d\alpha_Z} \right) \\ &= C_2 \left(\frac{d(\alpha_Z \text{rev}_Z)}{d\alpha_Z} - \frac{d(\alpha_n \text{rev}_n)}{d\alpha_n} \right) \end{aligned}$$

Hence, for $C_2 \neq 0$ each $\frac{d(\alpha_Z \text{rev}_Z)}{d\alpha_Z}$ has to be equal to $\frac{d(\alpha_n \text{rev}_n)}{d\alpha_n}$, i.e. all these derivatives have to be equal.



Table A2. Model parameters. Values correspond to FACE simulation experiment initial steady state for Optimal approach.

Symbol	Definition	Value	Unit
β_{NB}	C/N ratio of microbial biomass	11	g g^{-1}
$\beta_{N_{Enz}}$	C/N ratio of extracellular enzymes	3.1	g g^{-1}
β_{PB}	C/P ratio of microbial biomass	40	g g^{-1}
$\beta_{P_{Enz}}$	C/P ratio of extracellular enzymes	50	g g^{-1}
β_{P_m}	C/P ratio of a substrate at which the biomineralization decreased to 1/2	500	g g^{-1}
k_L	maximum decomposition rate of L	5.0	yr^{-1}
k_R	maximum decomposition rate of R	0.0318	yr^{-1}
a_E	enzyme production per microbial biomass	0.365	yr^{-1}
k_{mN}	product of enzyme half saturation constant and enzyme turnover	3.0	$\text{g m}^{-2} \text{yr}^{-1}$
τ	microbial biomass turnover rate	6.1	yr^{-1}
m	specific rate of maintenance respiration	5.84	yr^{-1}
ϵ	anabolic microbial C substrate efficiency	0.68	(-)
ϵ_{tvr}	microbial turnover that is not mineralized	0.3	(-)
ν_N	aggregated microbial organic N use efficiency	0.9	(-)
ν_P	aggregated microbial organic P use efficiency	0.0	(-)
i_{BN}	maximum microbial uptake rate of inorganic N	0.4	yr^{-1}
i_{BP}	maximum microbial uptake rate of inorganic P	100*	yr^{-1}
l_N	inorganic N leaching rate	0.96	yr^{-1}
l_P	inorganic P leaching rate	0.001*	yr^{-1}

* arbitrary high/low value so that system is not constrained by P

Table A3. Further symbols

Symbol	Definition	Unit
$S \in \{L, R\}$	Soil organic matter substrates, labile or residues	g m^{-2}
$Z \in \{L, R, P\}$	Enzyme classes for depolymerizing substrates L and R or biomineralizing phosphorus from both substrates	g m^{-2}
lim_E	Weight of limitation of microbial growth by element E (Wutzler et al., 2022, A15)	–
$d_{Zw}(\alpha_Z)$	Elemental-limitation-weighted return of enzyme Z	$\text{g m}^{-2} \text{yr}^{-1}$
d_Z	Elemental-limitation-weighted potential return for unlimited concentration of enzyme Z	$\text{g m}^{-2} \text{yr}^{-1}$
ω_{Enz}	Elemental-limitation factor for total enzyme synthesis in C units, $a_E B$	–
u_T	Total return = $\sum_Z d_{Zw}(\alpha_Z)$	$\text{g m}^{-2} \text{yr}^{-1}$
rev_Z	Revenue, i.e. return per investment, of enzyme Z	$\text{g m}^{-2} \text{yr}^{-1}$
syn_B	C for microbial biomass synthesis	$\text{g m}^{-2} \text{yr}^{-1}$

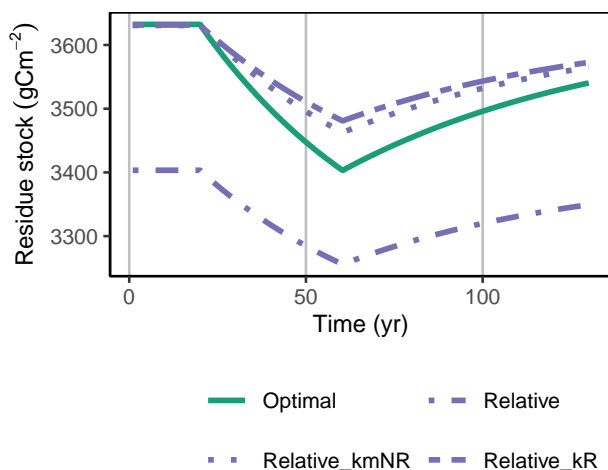


Figure B1. Relative approach simulated with a decreased decomposition rate of the residue pool, k_R or an increased k_{mNR} , in the FACE simulation experiment, matched the initial steady state stocks but still underestimated the decrease of residue stocks, R (gCm⁻²), during the period of higher carbon inputs.

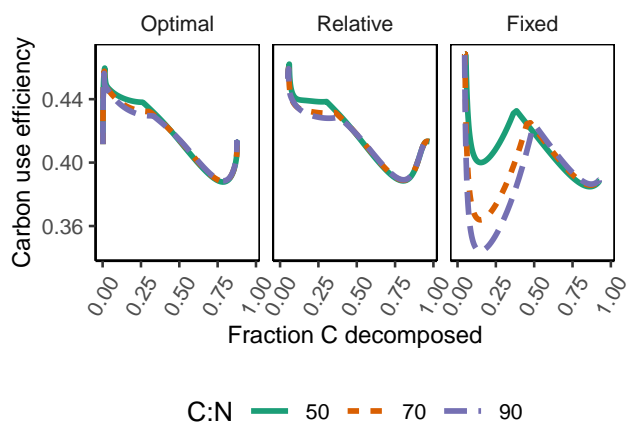


Figure B2. The differences in predicted carbon use efficiency (CUE) were small across optimization approaches (first two panels) compared to non-adaptive Fixed allocation in the Incubation simulation experiment.



C2 Total return of enzyme action

We seek the enzyme allocation α that maximizes the total limitation-weighted return, i.e. the action of enzymes, depolymerization and biomineralization. We exclude the trivial case of investing only into a single enzyme, ($\alpha_Z = 1$), and exclude enzymes that are not allocated to ($\alpha_Z = 0$).

340 The revenue of allocation to enzyme Z is $\text{rev}_Z = \frac{d_{Zw}(\alpha_Z)}{\alpha_Z \omega_{Enz} a_E B}$, where the return of enzyme Z , d_{Zw} , is a limitation-weighted flux of nutrients and carbon as detailed below. The investment is the share, α_Z , invested into production of enzyme Z multiplied by total limitation-weighted flux allocated to enzyme production, $\omega_{Enz} a_E B$.

The total return that is optimized is the the sum of each revenue multiplied by enzyme investment.

$$u_T = \omega_{Enz} a_E B \sum_Z \alpha_Z \text{rev}_Z \quad (\text{C1})$$

345 u_T fulfills the conditions of Lemma 1 (Appendix C1). Therefore, potential optima are located at the borders or at condition $\frac{d(\alpha_Z \text{rev}_Z)}{d\alpha_Z} = C_3$. Note that this conditions $\frac{du_T}{d\alpha_Z} = \omega_{Enz} a_E B \frac{d(\alpha_Z \text{rev}_Z)}{d\alpha_Z}$.

In the next section we restate the precise meaning of d_{Zw} and ω_{Enz} in SESAM that will be used in the following section to derive locations of potential optima expressed as a function of SESAM parameters.

C2.1 Depolymerizing enzymes

350 The return of an enzyme, E_Z , depolymerizing substrate, S_Z , is the elemental-limitation-weighted average of the returns for all elements.

$$d_{ZC} = k_Z S_Z \frac{\alpha a_E B}{k_{mNZ} + \alpha a_E B}$$

$$d_{ZN} = d_{ZC} / \beta_{NZ}$$

$$d_{ZP} = d_{ZC} / \beta_{PZ}$$

$$\begin{aligned} d_{Zw} &= w_C d_{ZC} \nu_{TC} + w_N d_{ZN} \nu_{TN} \beta_{NB} + w_P d_{ZP} \nu_{TP} \beta_{PB} \\ &= \frac{k_Z S_Z \alpha a_E B}{k_{mNZ} + \alpha a_E B} \left(w_C \nu_{TC} + w_N \nu_{TN} \frac{\beta_{NB}}{\beta_{NZ}} + w_P \nu_{TP} \frac{\beta_{PB}}{\beta_{PZ}} \right) \\ &= d_Z \frac{\alpha a_E B}{k_{mNZ} + \alpha a_E B} \end{aligned}$$

$$d_Z = k_Z S_Z \omega_Z$$

$$\omega_Z = w_C \nu_{TC} + w_N \nu_{TN} \frac{\beta_{NB}}{\beta_{NZ}} + w_P \nu_{TP} \frac{\beta_{PB}}{\beta_{PZ}}$$

w_E are weights for the strength of microbial growth limitation by elements C, N, and P. ν_{TE} are proportions of the mineralization that are actually taken up by microbial biomass. β_{EB} are C:E ratios of microbial biomass, and β_{EZ} are C:E ratios of mineralization flux, i.e. the source pool. d_Z is the potential return for saturating enzyme production, and ω_Z is the combined elemental weighting factor for the carbon mineralization flux.

355



Hence, the revenue for a depolymerizing enzyme and its derivative are

$$\begin{aligned} \text{rev}_Z(\alpha_Z) &= \frac{\text{return}}{\text{investment}} = \frac{d_Z w}{\alpha_Z \omega_{Enz} a_E B} \\ &= d_Z \frac{\alpha_Z a_E B}{k_{mNZ} + \alpha_Z a_E B} \frac{1}{\alpha_Z \omega_{Enz} a_E B} \\ &= \frac{d_Z}{\omega_{Enz}} \frac{1}{k_{mNZ} + \alpha_Z a_E B} \\ \frac{d(\alpha_Z \text{rev}_Z)}{d\alpha_Z} &= \frac{d_Z}{\omega_{Enz}} \frac{(k_{mNZ} + \alpha_Z a_E B) - \alpha_Z a_E B}{(k_{mNZ} + \alpha_Z a_E B)^2} \\ &= \frac{d_Z}{\omega_{Enz}} \frac{k_{mNZ}}{(k_{mNZ} + \alpha_Z a_E B)^2} \\ \omega_{Enz} &= w_C + w_N \frac{\beta_{NB}}{\beta_{NEnz}} + w_P \frac{\beta_{PB}}{\beta_{PEnz}} \end{aligned}$$

where ω_{Enz} is a weighting of the total carbon flux of enzyme production, $a_E B$, for current elemental limitation.

360 C2.2 Biomineralizing enzymes

The phosphatases only cleave phosphate groups from soil organic matter. Hence, they make available only P for uptake, without making available C and N. They attack both labile and residue organic matter. Although the P-cycle in SESAM will be described in its own manuscript, here, we state the important fluxes.

The potential return of action of P-degrading enzymes, d_P , includes the P-limitation weights w_P only, and does not divide by the C/P ratio of the substrate, as the mineralization flux is already expressed in P units:

$$d_P = \omega_P (k_{LP} l_{\beta_{PL}} L_P + k_{RP} l_{\beta_{PR}} R_P)$$

$$\omega_P = w_P \nu_P \beta_{PB}$$

$$l_{\beta_{PS}} = \frac{1}{1 + \beta_{PS}/\beta_{Pm}} = \frac{\beta_{Pm}}{\beta_{Pm} + \beta_{PS}}$$

where limitation factor $l_{\beta_{PS}} \in (0, 1)$ decreases the potential rate of a biomineralizing enzymes with increasing C/P ratio, β_{PS} , of substrate S . Parameter β_{Pm} is the C/P ratio at which the limitation factor decreased to 1/2.

Moreover, these phosphatases are also produced by plant roots at a rate e_P . Hence, one needs to calculate the return of microbe-produced enzymes that is additional to the return by plant-produced enzymes.

Return d_{Pm} , and revenue rev_P and its derivative are calculated as in Fig. C1.

The derivative of the total return with respect to the biomineralizing, enzyme, $\frac{d(\alpha_P \text{rev}_P)}{d\alpha_P}$, has the same form as the one of the depolymerizing enzyme (section C2.1). It, however, differs in the half-saturation constant of the Michaelis-Menten term which now includes the plant enzyme production: $(e_P + k_{mNP})$.

375 C3 Explicit optimum formulas

We seek the community composition, here represented by enzyme allocation, α , that maximizes total return. This maximizer is located either at the borders of the domain or at a location where all derivatives of the total return are zero. We only look at cases where we know which several enzymes take part in the mix with positive allocation, i.e. having $\alpha_Z \in (0, 1)$ and therefore do not need to look at the borders.

The strategy is first to find the small set of allocations where all the derivatives are zero, which includes maxima, minima, and saddle points. Second, we constrain the set to conditions $\alpha_Z \in (0, 1)$ and select that element that results in highest return.



$$\begin{aligned}
 d_{Pm} &= d_P \frac{e_P + \alpha_P a_E B}{k_{mNP} + e_P + \alpha_P a_E B} - d_P \frac{e_P}{k_{mNP} + e_P} \\
 &= d_P \frac{(e_P + \alpha_P a_E B)(k_{mNP} + e_P) - e_P(k_{mNP} + e_P + \alpha_P a_E B)}{(k_{mNP} + e_P + \alpha_P a_E B)(k_{mNP} + e_P)} \\
 &= d_P \frac{e_P k_{mNP} + \alpha_P a_E B k_{mNP} + e_P^2 + \alpha_P a_E B e_P - (e_P k_{mNP} + e_P^2 + \alpha_P a_E B e_P)}{(k_{mNP} + e_P)^2 + \alpha_P a_E B (k_{mNP} + e_P)} \\
 &= d_P \frac{\alpha_P a_E B k_{mNP}}{(k_{mNP} + e_P)^2 + \alpha_P a_E B (k_{mNP} + e_P)} \\
 &= d_P \frac{k_{mNP}}{e_P + k_{mNP}} \frac{\alpha_P a_E B}{(e_P + k_{mNP}) + \alpha_P a_E B} \\
 \text{rev}_P &= \frac{d_P}{\omega_{Enz}} \frac{k_{mNP}}{e_P + k_{mNP}} \frac{1}{(e_P + k_{mNP}) + \alpha_P a_E B} \\
 \frac{d(\alpha_P \text{rev}_P)}{d\alpha_P} &= \frac{d_P}{\omega_{Enz}} \frac{k_{mNP}}{e_P + k_{mNP}} \frac{d}{d\alpha_P} \left(\frac{\alpha_P}{(e_P + k_{mNP}) + \alpha_P a_E B} \right) \\
 &= \frac{d_P}{\omega_{Enz}} \frac{k_{mNP}}{e_P + k_{mNP}} \frac{(e_P + k_{mNP}) + \alpha_P a_E B - \alpha_P a_E B}{((e_P + k_{mNP}) + \alpha_P a_E B)^2} \\
 &= \frac{d_P}{\omega_{Enz}} \frac{k_{mNP}}{(e_P + k_{mNP} + \alpha_P a_E B)^2}
 \end{aligned}$$

Figure C1. Equations of return, revenue, and derivative for a biomineralizing enzyme

For simplifying formulas we make the assumption that all half-saturation parameters are equal: $k_{mNZ} = k_{mN}$.

C3.1 Two depolymerizing enzymes

Utilizing Lemma 1 (Appendix C1) we have:

$$\begin{aligned}
 \frac{d(\alpha_L \text{rev}_L)}{d\alpha_L} &= \frac{d(\alpha_R \text{rev}_R)}{d\alpha_R} \\
 \frac{d_L}{(k_{mN} + \alpha a_E B)^2} &= \frac{d_R}{(k_{mN} + (1 - \alpha) a_E B)^2}
 \end{aligned}$$

385 This provides a quadratic equation of α , which one can solve. We used the Sympy symbolic math tool.

That one of the two roots where $\alpha \in (0, 1)$ and that yields a higher $u_T(\alpha)$ provides the optimal α .

$$\alpha_{1,2} = \frac{a_E B d_L + k_{mN} (d_L + d_R) \pm \sqrt{d_L d_R (a_E B + 2k_{mN})}}{a_E B (d_L - d_R)}$$

C3.2 Depolymerizing and biomineralizing enzyme

$$\begin{aligned}
 \frac{d(\alpha_L \text{rev}_L)}{d\alpha_L} &= \frac{d(\alpha_P \text{rev}_P)}{d\alpha_P} \\
 \frac{d_L}{(k_{mN} + \alpha_L a_E B)^2} &= \frac{d_P}{((e_P + k_{mN}) + (1 - \alpha_L) a_E B)^2}
 \end{aligned}$$

$$390 \quad \alpha_{L1,2} = \frac{(a_E B + e_P + k_{mN}) d_L + k_{mN} d_P \pm \sqrt{d_L d_P (a_E B + e_P + 2k_{mN})}}{a_E B (d_L - d_P)}$$



$$\frac{d(\alpha_L \text{ rev}_L)}{d\alpha_L} = \frac{d(\alpha_R \text{ rev}_R)}{d\alpha_R} = \frac{d(\alpha_P \text{ rev}_P)}{d\alpha_P}$$

$$\frac{d_L}{(k_{mN} + \alpha a_E B)^2} = \frac{d_R}{(k_{mN} + (1 - \alpha - \alpha_P) a_E B)^2} = \frac{d_P}{((e_P + k_{mN}) + \alpha_P a_E B)^2}$$

We first compute α given α_P using the first equality. (see `sesam_LRP_deriv_sympy.py`)

$$\alpha_{L1,2} = \frac{a_E B(1 - \alpha_P)d_L + k_{mN}(d_L + d_R) \pm \sqrt{d_L d_R (a_E B(1 - \alpha_P) + 2k_{mN})}}{a_E B(d_L - d_R)}$$

Next we insert the both roots of $\alpha_L(\alpha_P)$ in equating the first and third utility to solve for α_P .

For the first root of α_L we get:

$$\alpha_{P1,2} = (A_1 \pm D_1)/B_1$$

$$A_1 = 2Bad_L^{\frac{3}{2}}d_P\sqrt{d_R} - Bad_L^2d_P - Bad_Ld_Pd_R + 4d_L^{\frac{3}{2}}d_P\sqrt{d_R}k_{mN} - d_L^3e_P - d_L^3k_{mN}$$

$$- 2d_L^2d_Pk_{mN} + 2d_L^2d_Re_P + 2d_L^2d_Rk_{mN} - 2d_Ld_Pd_Rk_{mN} - d_Ld_R^2e_P - d_Ld_R^2k_{mN}$$

$$D_1 = \sqrt{d_P(Ba + e_P + 3k_{mN})} \sqrt{-2d_L^{\frac{9}{2}}\sqrt{d_R} + 4d_L^{\frac{7}{2}}d_R^{\frac{3}{2}} - 2d_L^{\frac{5}{2}}d_R^{\frac{5}{2}} + d_L^5 - d_L^4d_R - d_L^3d_R^2 + d_L^2d_R^3}$$

$$B_1 = Ba \left(2d_L^{\frac{3}{2}}d_P\sqrt{d_R} + d_L^3 - d_L^2d_P - 2d_L^2d_R - d_Ld_Pd_R + d_Ld_R^2 \right)$$

For the second root of α_L we get:

$$\alpha_{P3,4} = (A_2 \pm D_2)/B_2$$

$$A_2 = 2Bad_L^{\frac{3}{2}}d_P\sqrt{d_R} + Bad_L^2d_P + Bad_Ld_Pd_R + 4d_L^{\frac{3}{2}}d_P\sqrt{d_R}k_{mN} + d_L^3e_P + d_L^3k_{mN}$$

$$+ 2d_L^2d_Pk_{mN} - 2d_L^2d_Re_P - 2d_L^2d_Rk_{mN} + 2d_Ld_Pd_Rk_{mN} + d_Ld_R^2e_P + d_Ld_R^2k_{mN}$$

$$D_2 = \sqrt{d_P(Ba + e_P + 3k_{mN})} \sqrt{2d_L^{\frac{9}{2}}\sqrt{d_R} - 4d_L^{\frac{7}{2}}d_R^{\frac{3}{2}} + 2d_L^{\frac{5}{2}}d_R^{\frac{5}{2}} + d_L^5 - d_L^4d_R - d_L^3d_R^2 + d_L^2d_R^3}$$

$$B_2 = Ba \left(2d_L^{\frac{3}{2}}d_P\sqrt{d_R} - d_L^3 + d_L^2d_P + 2d_L^2d_R + d_Ld_Pd_R - d_Ld_R^2 \right)$$

Figure C2. Potential optima for Two depolymerizing and one biomineralizing enzyme

C3.3 Two depolymerizing and one biomineralizing enzyme

We set $\alpha_R = 1 - \alpha - \alpha_P$ and have equations of Fig. C2.

The products of the single parameters are the same as with $\alpha_{P1,2}$, but they are combined with different signs.

That one of the four roots where $\alpha_P \in (0,1)$ and derived $\alpha_L(\alpha_P) \in (0,1)$ and that yields a highest $u_T(\alpha)$ provides the

395 optimal α .



C4 Excursion: replacing revenue by relative profit

Revenue, here, is defined as return per investment, $\text{rev}_Z = d_{Zw}/\text{inv}_{Zw}$. One could argue that one should rather optimize the profit, i.e. return - investment, or the relative profit, rev_{pZ} , i.e. profit/investment. Here we show, that optimizing the profit yields the same optimal allocation as optimizing the return.

$$400 \quad \text{rev}_{pZ} = (d_{Zw} - \text{inv}_{Zw})/\text{inv}_{Zw} = \text{rev}_Z - 1$$

$$\frac{d(\alpha_Z \text{rev}_{pZ})}{d\alpha_Z} = \frac{d(\alpha_Z \text{rev}_Z)}{d\alpha_Z} - \frac{d\alpha_Z}{d\alpha_Z} = \frac{d(\alpha_Z \text{rev}_Z)}{d\alpha_Z} - 1$$

The total profit is the sum of relative profits multiplied by total enzyme investment, inv_w .

$$u_{Tp}(\alpha) = \text{inv}_w \sum_Z \alpha_Z \text{rev}_{pZ}(\alpha_Z)$$

This equation fulfills the conditions of Lemma 1 (Appendix C1) and at the optima all derivatives are equal.

$$\frac{d(\alpha_i \text{rev}_{p_i})}{d\alpha_i} = \frac{d(\alpha_j \text{rev}_{p_j})}{d\alpha_j}$$

$$\frac{d(\alpha_i \text{rev}_i)}{d\alpha_i} - 1 = \frac{d(\alpha_j \text{rev}_j)}{d\alpha_j} - 1$$

$$\frac{d(\alpha_i \text{rev}_i)}{d\alpha_i} = \frac{d(\alpha_j \text{rev}_j)}{d\alpha_j}$$

405 Hence, optimizing profits yields the same conditions as optimizing returns.

Appendix D: Derivation of the relative approach

The Relative approach estimates optimal allocation to be proportional to revenue (2.2.2). Hence, we seek the conditions for which the following relationship holds:

$$\frac{\alpha_j}{\alpha_i} \approx \frac{\text{rev}_j}{\text{rev}_i}$$

410 At the solution of the Optimal approach all the derivatives of (revenue times α) for all enzymes in the mix are equal (Appendix C2). With using $\frac{d(\alpha_Z \text{rev}_Z)}{d\alpha_Z} \approx \text{rev}_Z \frac{e_Z + k_m N_Z}{\alpha_Z a_E B}$, as shown below, for any two enzymes i, j we have:



$$\begin{aligned} \frac{d(\alpha_i \text{rev}_i)}{d\alpha_i} &= \frac{d(\alpha_j \text{rev}_j)}{d\alpha_j} \\ \text{rev}_i \frac{e_i + k_{mNi}}{\alpha_i a_{EB}} &\approx \text{rev}_j \frac{e_j + k_{mNj}}{\alpha_j a_{EB}} \\ \frac{\alpha_j}{\alpha_i} &\approx \frac{\text{rev}_j e_j + k_{mNj}}{\text{rev}_i e_i + k_{mNi}} \\ \frac{\alpha_j}{\alpha_i} &\approx \frac{\text{rev}_j}{\text{rev}_i} \end{aligned}$$

The last approximation holds only for similar half-saturation parameters across enzymes $k_{mNZ} \approx k_{mN}$, and plant enzyme production being low compared to this half-saturation: $e_Z \ll k_{mN}$.

415 The first approximation in the second line is only valid for enzyme production flux is not larger than the half-saturation, k_{mNZ} (see below). This is violated at low microbial biomass or very low α_Z .

Hence, the optimal allocation is approximately proportional to the revenue for the combination of the following conditions:

- all enzymes have a non-negligible share
- microbial biomass is sufficiently high
- 420 – plant biomineralizing enzyme production is low.

The derivation above used the following relationship that still needs to be shown: $\frac{d(\alpha_Z \text{rev}_Z)}{d\alpha_Z} \approx \text{rev}_Z \frac{e_Z + k_{mNZ}}{\alpha_Z a_{EB}}$.

For depolymerizing enzymes we use the following approximations. For $\alpha_Z a_{EB} \gg k_{mNZ}$, i.e. $2k_{mNZ} + \alpha_Z a_{EB} \approx \alpha_Z a_{EB}$, the half-saturation k_{mNZ} can be neglected in the denominator of the revenue. Note that $\alpha_Z a_{EB} \gg k_{mNZ}$ implies $(\alpha_Z a_{EB})^2 \gg k_{mNZ}^2$.

$$\begin{aligned} \text{rev}_Z &= \frac{d_Z}{\omega_{Enz}} \frac{1}{k_{mNZ} + \alpha_Z a_{EB}} \\ &\approx \frac{d_Z}{\omega_{Enz}} \frac{1}{\alpha_Z a_{EB}} \\ \frac{d(\alpha_Z \text{rev}_Z)}{d\alpha_Z} &= \frac{d_Z}{\omega_{Enz}} \frac{k_{mNZ}}{(k_{mNZ} + \alpha_Z a_{EB})^2} \\ 425 &= \frac{d_Z}{\omega_{Enz}} \frac{k_{mNZ}}{k_{mNZ}^2 + 2k_{mNZ}\alpha_Z a_{EB} + (\alpha_Z a_{EB})^2} \\ &\approx \frac{d_Z}{\omega_{Enz}} \frac{k_{mNZ}}{\alpha_Z a_{EB}(2k_{mNZ} + \alpha_Z a_{EB})} \\ &= \text{rev}_Z \frac{k_{mNZ}}{2k_{mNZ} + \alpha_Z a_{EB}} \\ &\approx \text{rev}_Z \frac{k_{mNZ}}{\alpha_Z a_{EB}} \end{aligned}$$

where the first two relationships have been derived in Appendix C2.1. Since depolymerizing enzymes are not produced by plant roots, $e_Z = 0$.



Similarly, for biomineralizing enzymes we require $\alpha_Z a_E B \gg k_{mNZ} + e_Z$, where e_Z is the production of enzyme Z by plants.

$$\begin{aligned}
 \text{rev}_Z &= \frac{d_Z}{\omega_{Enz}} \frac{k_{mNZ}}{e_Z + k_{mNZ}} \frac{1}{e_Z + k_{mNZ} + \alpha_Z a_E B} \\
 &\approx \frac{d_Z}{\omega_{Enz}} \frac{k_{mNZ}}{e_Z + k_{mNZ}} \frac{1}{\alpha_Z a_E B} \\
 \frac{d(\alpha_Z \text{rev}_Z)}{d\alpha_Z} &= \frac{d_Z}{\omega_{Enz}} \frac{k_{mNZ}}{(e_Z + k_{mNZ} + \alpha_Z a_E B)^2} \\
 430 \quad &= \frac{d_Z}{\omega_{Enz}} \frac{k_{mNZ}}{(e_Z + k_{mNZ})^2 + 2(e_Z + k_{mNZ})\alpha_Z a_E B + (\alpha_Z a_E B)^2} \\
 &\approx \frac{d_Z}{\omega_{Enz}} \frac{k_{mNZ}}{\alpha_Z a_E B (2(e_Z + k_{mNZ}) + \alpha_Z a_E B)} \\
 &= \text{rev}_Z \frac{e_Z + k_{mNZ}}{2(e_Z + k_{mNZ}) + \alpha_Z a_E B} \\
 &\approx \text{rev}_Z \frac{e_Z + k_{mNZ}}{\alpha_Z a_E B}
 \end{aligned}$$

Appendix E: Derivative-based change of community allocation

SESAM assumes that microbial community develops in a way to optimize growth of the entire community. Growth increases with uptake, i.e. the total limitation-weighted return, i.e. decomposition and depolymerization flux, for given enzyme allocation. The revenue of allocation to enzyme Z is $\text{rev}_Z = \frac{d_{Zw}(\alpha_Z)}{\alpha_Z \omega_{Enz} a_E B}$. The return d_{Zw} is a limitation-weighted mineralization flux or uptake flux of nutrients and carbon (sections C2.1 and C2.2). The investment is the share, α_Z , invested into production of enzyme Z multiplied by total limitation-weighted flux, $\omega_{Enz} a_E B$, allocated to enzyme production.

Although its possible to derive explicit formula for the allocation that optimizes total return for simple cases, the formulas quickly grow and involve higher-order polynomials of α with several solutions outside the reasonable bound $\alpha_Z \in [0, 1]$.

Here we follow an alternative local approach were we assume the rate change of α_Z over time to be proportional to the deviation of the derivative of change of total return with respect to α_Z to the average across the derivatives for different enzymes. The higher the increase in total return for shifting allocation towards a specific enzyme, the faster the community changes in this direction.

The total return is a weighted sum of enzyme revenues, and derivatives of $\frac{d(\alpha_Z \text{rev}_Z)}{d\alpha_Z}$ have been derived for depolymerizing and biomineralizing enzymes (section C2).

$$\begin{aligned}
 u_T &= \omega_{Enz} a_E B \sum_Z \alpha_Z \text{rev}_Z(\alpha_Z) \\
 445 \quad \frac{du_T}{d\alpha_Z} &= \omega_{Enz} a_E B \sum_Z \frac{d(\alpha_Z \text{rev}_Z)}{d\alpha_Z}
 \end{aligned}$$



We assume that the larger the change in return with increasing allocation, i.e. the derivative to allocation coefficient α_Z , the larger is the change in allocation. In addition to the assumption of proportionality to the derivative, we assume that the community changes at a rate of the same magnitude as synthesis and turnover of microbial biomass.

$$\begin{aligned} \frac{d\alpha_Z}{dt} &\propto \frac{du_T}{d\alpha_Z} - m_{du} \\ &= \left(\frac{|\text{syn}_B|}{B} + \tau \right) \frac{\frac{du_T}{d\alpha_Z} - m_{du}}{m_{du}} \\ m_{du} &= \text{mean}_i \left(\frac{du_T}{d\alpha_i} \right) \end{aligned}$$

450 where m_{du} is the average across derivatives of return across enzymes that are allocated to. If all changes are the same, i.e. equal to the mean, the allocation is optimal because it does not increase in any direction.

We want the change to be proportional to the change in return compared to the average return. Subtracting this mean ensures that the sum of all the changes in α sums to zero so that the sum across α is preserved. The proportionality factor normalizes the change in return and multiplies this relative change by the rate of microbial turnover, composed of biomass synthesis and
455 biomass turnover.

E1 Exclude enzymes whose negative relative change is larger than its share

Community may not allocate to all enzymes. Hence, m_{due} (an updated version of m_{du}) averages only across a subset of enzymes. The derivative optimization strategy assumes that nothing is allocated to an enzyme if its normalized change towards zero is larger than than its current share, i.e. is more negative than $-\alpha_Z$.

$$\begin{aligned} Z_0 &= \left\{ Z \mid \frac{\frac{du_T}{d\alpha_Z} - m_{due}}{m_{due}} < -\alpha_Z \right\} \\ \frac{d\alpha_Z}{dt} &= \left(\frac{|\text{syn}_B|}{B} + \tau \right) \begin{cases} -\alpha_Z & \text{for } Z \in Z_0 \\ \frac{\frac{du_T}{d\alpha_Z} - m_{due}}{m_{due}} & \text{otherwise} \end{cases} \\ &= \left(\frac{|\text{syn}_B|}{B} + \tau \right) \max \left(\frac{\frac{du_T}{d\alpha_Z} - m_{due}}{m_{due}}, -\alpha_Z \right) \\ m_{due} &= \frac{\sum_{\zeta \notin Z_0} \frac{du_T}{d\alpha_\zeta}}{|\{Z\} \setminus Z_0| + \sum_{\zeta \in Z_0} \alpha_\zeta} \end{aligned}$$

460

Where $|\{Z\} \setminus Z_0|$ denotes the number of enzymes allocated to, i.e. the cardinality of the set of all enzymes without those in Z_0 . The relative change of those excluded enzymes is set to $-\alpha_Z$, resulting in negative changes going to zero as α_Z approaches zero. Hence, the relative change is lower-bounded by $-\alpha_Z$.



m_{du} has to be adjusted to m_{due} , so that $\sum_i \frac{d\alpha_i}{dt} = 0$ holds.

$$465 \quad \sum_{\zeta \notin Z_0} \frac{\frac{du_T}{d\alpha_Z} - m_{due}}{m_{due}} + \sum_{\zeta \in Z_0} -\alpha_\zeta = 0$$

This definition is recursive, because m_{due} is computed across a set that is defined using m_{due} . In order to determine Z_0 one can start with the empty set and add all enzymes that fulfill the condition. If enzymes were added then the mean across remaining derivatives increases, and the condition has to be checked again. Hence, adding enzymes to Z_0 is repeated until no more enzymes fulfill the condition and the mean does not change any more.

470 *Author contributions.* TW and CR developed the math, TW implemented it into the model, and led the writing of the manuscript. TW, CR, BA, and MS contributed to the discussion of results and writing of the manuscript

Competing interests. The contact author has declared that none of the authors has any competing interests.

Acknowledgements. We thank Lin Yu for fruitful discussion. We thank the Max Planck Society for funding.



References

- 475 Calabrese, S., Mohanty, B. P., and Malik, A. A.: Soil microorganisms regulate extracellular enzyme production to maximize their growth rate, *Biogeochemistry*, 158, 303–312, <https://doi.org/10.1007/s10533-022-00899-8>, 2022.
- Carvalhais, L. C., Dennis, P. G., Tyson, G. W., and Schenk, P. M.: Application of metatranscriptomics to soil environments, *Journal of Microbiological Methods*, 91, 246–251, <https://doi.org/10.1016/j.mimet.2012.08.011>, 2012.
- Dewar, R. C.: Maximum entropy production and plant optimization theories, *Philosophical Transactions of the Royal Society B: Biological Sciences*, 365, 1429–1435, <https://doi.org/10.1098/rstb.2009.0293>, 2010.
- 480 Feng, X., Lu, Y., Jiang, M., Katul, G., Manzoni, S., Mrad, A., and Vico, G.: Instantaneous stomatal optimization results in suboptimal carbon gain due to legacy effects, *Plant, Cell & Environment*, 45, 3189–3204, <https://doi.org/10.1111/pce.14427>, 2022.
- Heitkötter, J. and Marschner, B.: Soil zymography as a powerful tool for exploring hotspots and substrate limitation in undisturbed subsoil, *Soil Biology and Biochemistry*, 124, 210–217, <https://doi.org/10.1016/j.soilbio.2018.06.021>, 2018.
- 485 Herold, N., Schöning, I., Michalzik, B., Trumbore, S., and Schrumpf, M.: Controls on soil carbon storage and turnover in German landscapes, *Biogeochemistry*, 119, 435–451, <https://doi.org/10.1007/s10533-014-9978-x>, 2014.
- Hungate, B. A., Mau, R. L., Schwartz, E., Caporaso, J. G., Dijkstra, P., van Gestel, N., Koch, B. J., Liu, C. M., McHugh, T. A., Marks, J. C., Morrissey, E. M., and Price, L. B.: Quantitative Microbial Ecology through Stable Isotope Probing, *Applied and Environmental Microbiology*, 81, 7570–7581, <https://doi.org/10.1128/aem.02280-15>, 2015.
- 490 Kaiser, C., Franklin, O., Dieckmann, U., and Richter, A.: Microbial community dynamics alleviate stoichiometric constraints during litter decay, *Ecology Letters*, 17, 680–690, <https://doi.org/10.1111/ele.12269>, 2014.
- Kozjek, K., Manoharan, L., Urich, T., Ahrén, D., and Hedlund, K.: Microbial gene activity in straw residue amendments reveals carbon sequestration mechanisms in agricultural soils, *Soil Biology and Biochemistry*, 179, 108 994, <https://doi.org/10.1016/j.soilbio.2023.108994>, 2023.
- 495 Kuzyakov, Y., Friedel, J. K., and Stahr, K.: Review of mechanisms and quantification of priming effects, *Soil Biology & Biochemistry*, 32, 1485–1498, 2000.
- Lehmann, J. and Kleber, M.: The contentious nature of soil organic matter, *Nature*, 528, 60–68, <https://doi.org/10.1038/nature16069>, 2015.
- Manzoni, S.: Flexible Carbon-Use Efficiency across Litter Types and during Decomposition Partly Compensates Nutrient Imbalances—Results from Analytical Stoichiometric Models, *Frontiers in Microbiology*, 8, <https://doi.org/10.3389/fmicb.2017.00661>, 2017.
- 500 Manzoni, S., Čapek, P., Mooshammer, M., Lindahl, B. D., Richter, A., and Šantrůčková, H.: Optimal metabolic regulation along resource stoichiometry gradients, *Ecology Letters*, 20, 1182–1191, <https://doi.org/10.1111/ele.12815>, 2017.
- Manzoni, S., Chakrawal, A., Spohn, M., and Lindahl, B. D.: Modeling Microbial Adaptations to Nutrient Limitation During Litter Decomposition, *Frontiers in Forests and Global Change*, 4, <https://doi.org/10.3389/ffgc.2021.686945>, 2021.
- Manzoni, S., Chakrawal, A., and Ledder, G.: Decomposition rate as an emergent property of optimal microbial foraging, *Frontiers in Ecology and Evolution*, 11, <https://doi.org/10.3389/fevo.2023.1094269>, 2023.
- 505 Marx, M.-C., Wood, M., and Jarvis, S.: A microplate fluorimetric assay for the study of enzyme diversity in soils, *Soil Biology and Biochemistry*, 33, 1633–1640, [https://doi.org/10.1016/s0038-0717\(01\)00079-7](https://doi.org/10.1016/s0038-0717(01)00079-7), 2001.
- Mooshammer, M., Wanek, W., Hämmerle, I., Fuchslueger, L., Hofhansl, F., Knoltsch, A., Schneckner, J., Takriti, M., Watzka, M., Wild, B., Keiblinger, K. M., Zechmeister-Boltenstern, S., and Richter, A.: Adjustment of microbial nitrogen use efficiency to carbon:nitrogen imbalances regulates soil nitrogen cycling, *Nature Communications*, 5, <https://doi.org/10.1038/ncomms4694>, 2014a.
- 510



- Mooshammer, M., Wanek, W., Zechmeister-Boltenstern, S., and Richter, A.: Stoichiometric imbalances between terrestrial decomposer communities and their resources: mechanisms and implications of microbial adaptations to their resources, *Frontiers in Microbiology*, 5, <https://doi.org/10.3389/fmicb.2014.00022>, 2014b.
- 515 Perveen, N., Barot, S., Alvarez, G., Klumpp, K., Martin, R., Rapaport, A., Herfurth, D., Louault, F., and Fontaine, S.: Priming effect and microbial diversity in ecosystem functioning and response to global change: a modeling approach using the SYMPHONY model, *Global Change Biology*, 20, 1174 – 1190, <https://doi.org/10.1111/gcb.12493>, 2014.
- Richter, A.: What controls carbon and nutrient cycling in soil? Microbial growth as the fundamental driver of soil biogeochemistry., <https://doi.org/10.5194/egusphere-egu23-10907>, 2023.
- 520 Robert W. Sterner, J. J. E.: *Ecological stoichiometry: the biology of elements from molecules to the biosphere*, Princeton University Press, 2002.
- Schimel, J. P. and Weintraub, M. N.: The implications of exoenzyme activity on microbial carbon and nitrogen limitation in soil: a theoretical model, *Soil Biology and Biochemistry*, 35, 549–563, 2003.
- Spohn, M., Carminati, A., and Kuzyakov, Y.: Soil zymography – A novel in situ method for mapping distribution of enzyme activity in soil, *Soil Biology and Biochemistry*, 58, 275–280, <https://doi.org/10.1016/j.soilbio.2012.12.004>, 2013.
- 525 Strogatz, S. H.: *Nonlinear dynamics and chaos: with applications to physics, Biology, Chemistry and Engineering*, p. 1, 1994.
- Tang, J. and Riley, W. J.: Competitor and substrate sizes and diffusion together define enzymatic depolymerization and microbial substrate uptake rates, *Soil Biology and Biochemistry*, 139, 107 624, <https://doi.org/10.1016/j.soilbio.2019.107624>, 2019.
- Wutzler, T. and Reichstein, M.: Colimitation of decomposition by substrate and decomposers - a comparison of model formulations, *Biogeosciences*, 5, 749–759, <https://doi.org/10.5194/bg-5-749-2008>, 2008.
- 530 Wutzler, T., Zaehle, S., Schrumpf, M., Ahrens, B., and Reichstein, M.: Adaptation of microbial resource allocation affects modelled long term soil organic matter and nutrient cycling, *Soil Biology and Biochemistry*, 115, 322–336, <https://doi.org/10.1016/j.soilbio.2017.08.031>, 2017.
- Wutzler, T., Yu, L., Schrumpf, M., and Zaehle, S.: Simulating long-term responses of soil organic matter turnover to substrate stoichiometry by abstracting fast and small-scale microbial processes: the Soil Enzyme Steady Allocation Model (SESAM; v3.0), *Geoscientific Model Development*, 15, 8377–8393, <https://doi.org/10.5194/gmd-15-8377-2022>, 2022.
- 535